Journal of Molecular Liquids 218 (2016) 83–94

Contents lists available at ScienceDirect

Journal of Molecular Liquids

journal homepage: www.elsevier.com/locate/molliq

The study of solute–solvent interactions in 1-ethyl-3-methylimidazolium ethylsulfate + 2-ethoxyethanol from density, speed of sound and refractive index measurements

Srinivasa Reddy M [a,e], Md Nayeem Sk [b], Raju K.T.S.S. [c], Srinivasa Rao V [d], Hari Babu B. [e,*]

[a] Department of Chemistry, KRK Govt. Degree College, Addanki-523201, Andhra Pradesh, India
[b] Department of Physics, KRK Govt. Degree College, Addanki-523201, Andhra Pradesh, India
[c] Department of Chemistry, Andhra Loyola College, Vijayawada -520008, Andhra Pradesh, India
[d] Department of Chemistry, S.R.R&CVR Govt. Degree College, Vijayawada -520 004, A.P., Andhra Pradesh, India
[e] Department of Chemistry, Acharya Nagarjuna University, Nagarjunanagar–522510, Andhra Pradesh, India

ARTICLE INFO

Article history:
Received 5 November 2015
Accepted 30 January 2016
Available online xxxx

Keywords:
[Emim][EtSO$_4$]
2-ethoxyethanol
Density
Speed of sound
Refractive index
Excess/deviation parameters

ABSTRACT

Physical properties, such as density (ρ), speed of sound (u) and refractive index (n_D) for pure [Emim][EtSO$_4$], 2-ethoxyethanol and their binary mixtures are measured using Anton Paar vibrating tube density, sound velocity meter (DSA 5000 M) and automatic refract meter over the whole composition range as a function of temperature between (298.15–328.15) K at atmospheric pressure. Experimental values were used to calculate the excess molar volumes (V_m^E), excess values of partial molar volumes ($\overline{V}_m^E$), partial molar volumes at infinite dilution ($\overline{V}_m^{E,\infty}$), excess/deviation values of isentropic compressibility (κ_s^E), isothermal compressibility (κ_T^E), free length (L_f^E), speed of sound (u^E), refractive index ($\Delta_\phi n_D$), internal pressure (π_i^E), free volume (V_f^E) and isobaric thermal expansion coefficient (α_p^E) for the binary mixtures. These excess/deviation properties were fitted to the Redlich–Kister type equation to obtain the binary coefficients and the standard deviations. A qualitative analysis of these parameters indicates strong intermolecular interactions between the liquids in study. This was further supported by IR spectroscopy.

1. Introduction

Ionic liquids (ILs) as 'green' solvents and alternative to traditional organic solvents are found increasing their utilization in many areas of technology and science such as synthesis, catalysis, biocatalysts, electrochemical devices, separation technology, as reaction media, as green solvents and in biodegradable materials [1–9]. ILs can be chosen to have different anions and cations so that one can form IL with the desired properties. Especially, some kinds of ILs with special functional groups have been designed for application in many industrial processes. They consist entirely of cations and anions, with negligible vapor pressure [10], good thermal stability and broad liquid temperature ranges [11–13], and non-flammability [14–18]. The salt form and extremely low vapor pressure features garnered them much recent attention as potential solvents to replace volatile organic solvents in a wide variety of chemical reactions, separations, and manufacturing processes.

The potential of these new substances can be exploited with experimental methods that can reliably predict the thermodynamic properties of ionic liquids and their mixtures with other molecular solvents. Most of these novel media are characterized by their volumetric, acoustic and refractive index properties, since these data are significant for industrial applications. ILs have been considered: solvents for reactions, absorption media for CO_2 capture [19,20], the separating agent in extractive distillation [21–23], heat transfer fluids [24–26], for processing biomass [27], and the working fluid in a variety of electrochemical applications [28]. Many technological processes involving ILs require the knowledge of thermophysical properties of mixing them with organic molecular solvents. To understand the interactions of their constituting cations and anions with the molecular solvents, the behavior of ILs when mixed with molecular organic solvents is of utmost importance. The IL in the investigation, 1-ethyl-3-methylimidazolium ethyl sulfate {[Emim][EtSO$_4$]} which is used as extracting solvent for the removal of many organic compounds through liquid–liquid extraction [29,30]. It is also widely used in enzyme catalysis in ionic liquids [31], in chromatography [32], etc. On the other hand, alkoxyethanols, which are amphiphilic organic solvents have been used in many chemical processes. The mixtures containing alkoxyethanols are very important from theoretical point of view, not only of their self-association, but also due to the strong intermolecular effects produced by the presence of –O– and –OH groups in the same molecule. It is of great importance to understand the mixing behavior of ILs in alkoxyethanols and to provide accurate physicochemical data. Therefore some researchers studied the thermodynamic behavior of the mixtures of ILs with alkoxyethanols [33–

* Corresponding author.

http://dx.doi.org/10.1016/j.molliq.2016.01.096
0167-7322/

36].The solvent, 2-ethoxyethanol is not only used as solvent in organic synthesis but also in paints, coatings, inks, cleaners, polishes, brake fluids and jet fuels. This can also be used to find wide applications such as chemical intermediate and solvent coupler of mixtures and water-based formulations [37]. Therefore, with this wide range of industrial applications of [Emim][$EtSO_4$] and 2-ethoxyethanol individually, encouraged us to measure the thermophysical properties and understand its interaction behavior.

Systematic investigation of the physicochemical properties of [Emim][$EtSO_4$] with molecular organic solvents including water, methanol, ethanol, 1-propanol, 2-propanol, acetone, acetonitrile, propylene carbonate, dichloromethane and sugars has been reported. González et al. [38] reported the densities, speed of sound and refractive indices of [Emim][$EtSO_4$] binary mixtures with methanol, 1-propanol, and 2-propanol, whereas Miaja et al. [39] reported the density data of binary mixtures of [Emim][$EtSO_4$] with water. On the other hand, Lehmann et al. [40] reported the density data of acetone, acetonitrile, propylene carbonate, dichloromethane, methanol, ethanol, and water binary mixtures with [Emim][$EtSO_4$], whereas Domańska et al. [41] reported the density data of binary solutions of [Emim][$EtSO_4$] with water and ethanol. Aristides et al. [42] reported density data of [Emim][$EtSO_4$] binary mixtures with sugars. Ramalingam et al. [43] studied the interactions of [Emim][$EtSO_4$] with aromatic sulfur species. But the thermoacoustic, volumetric and refractive index data of [Emim][$EtSO_4$] with 2-ethoxyethanol was not reported.

On the basis of our preliminary experiments, 1-ethyl-3-methylimidazoliumte ethyl sulfate {[Emim][$EtSO_4$]}has been found to be totally miscible with 2-ethoxyethanol at all proportions. Hence, in the present study, it is proposed to measure the physical properties (densities, ρ, speed of sound, u, refractive indices, n_D) of the binary mixtures of [Emim][$EtSO_4$] with 2-ethoxyethanol in the temperature range from (298.15 to 328.15) K, over the whole composition range and to estimate their excess/deviation properties for their potential application in industrial processes. On the basis of the measured values, thermodynamic and acoustical excess/deviation parameters such as molar volumes, V_m^E, isentropic compressibility(κ_s^K), isothermal compressibility (κ_T^E), free length (L_f^E), speed of sound (u^E), refractive index on volume fraction basis, $\Delta_\phi n_D$, internal pressure (π_i^E), free volume (V_f^E) and isobaric thermal expansion coefficient (α_p^E) have been determined for the binary mixtures and fitted using Redlich–Kister type polynomial equation.

2. Experimental

2.1. Chemicals

The ionic liquid, 1-Ethyl-3-methylimidazolium ethyl sulfate, or [Emim][$EtSO_4$](CAS 342573-75-5) with purity 0.99 in mass fraction used in this work. It was purchased from Iolitec GmBH (Germany), while the 2-ethoxyethanol (CAS110-80-5) was supplied by Sigma-Aldrich. The chemicals used in the study were purified by the methods described in literature [48]. The suppliers and the purity for pure compounds are reported in Table 1. The water content in investigated IL and 2-ethoxyethanol was determined using a Karl Fischer titrator (Metrohm, 890 Titrando). Before any measurements, all samples were dried for at least 72 h under a vacuum (0.1 Pa) and moderate temperature (beginning at room temperature and increasing it gradually over a 6-h period up to 333 K). The water content of all the samples was further checked and found to be in the range of less than 50 ppm, a value much lower than the original pre-evacuation analysis, which typically showed values in the range of less than 210 ppm. [Emim][$EtSO_4$] is used without further purification, 2-ethoxyethanol is further purified by distillation and the purities were verified by comparing the measured density, speed of sound and refractive index of the pure liquids with the literature at atmospheric pressure are given in Table 2.

2.2. Apparatus and procedure

2.2.1. Sample preparation

All samples were freshly prepared in Amber glass vials with screw caps having PFE septa, and a secure sealed with parafilm to prevent the absorption of moisture from the atmosphere, and was then stirred for more than 30 min to ensure total dissolution of the mixtures. Samples were taken from the vials with a syringe through the PFE septum. The mass of the dry bottle was first determined. The less volatile component (RTIL) of the mixture was introduced in the bottle and mass was recorded. The other component (organic liquid) was added and the mass of bottle including two components was determined. Samples were prepared by weighing with a precision of ± 0.01 mg, using a Sartorius electronic balance. The uncertainty of the resulting mole fractions of the mixtures was estimated as being $\pm 1 \times 10^{-5}$.

2.2.2. Measurement of density and speed of sound

Densities and speed of sound were measured with an Anton Paar DSA-5000 M vibrating tube density and sound velocity meter with a resolution of $\pm 5 \times 10^{-5}$ cm^{-3}. The density meter was calibrated with doubly distilled degassed water, and with dry air at atmospheric pressure. The temperature of the apparatus was controlled to within ± 0.01 K by a built-in Peltier device that corresponds to an uncertainty in density of $\pm 0.0002\%$. Measured density values are precise to 1×10^{-5} g cm^{-3}. The experimental uncertainties for density and speed of sound are $\pm 3 \times 10^{-5}$ g cm^{-3} and ± 0.3 ms^{-1} respectively. The uncertainty estimates do not include the effects of certain minor impurities that may be present in the ionic liquid.

2.2.3. Measurement of refractive index

The refractive indices were determined using an automatic refract meter supplied by Anton Paar which is having a temperature controller that keeps the samples at working temperature. The uncertainties in the temperature and refractive index values are ± 0.01 K and $\pm 4 \times 10^{-5}$, respectively. The apparatus was calibrated by measuring the refractive index of millipore quality water and tetrachloroethylene (supplied by the company) before each series of measurements according to manual instructions. The calibration was checked with pure liquids with known refractive index.

2.2.4. Measurement of infrared spectra

Infrared transmittance was measured by making use of Shimadzu Fourier transform infrared (FT-IR) spectrometer, equipped with attenuated total reflectance (ATR) accessories. A fixed cell about 0.1 mm thickness is used which is suitable for the measurement of volatile samples also. The spectral region is 650–4000 cm^{-1} with resolution 2 cm^{-1} and 100 scans. At least five repeated measurements were performed for each sample.

Table 1
List of chemicals with details of provenance, CAS number, and mass fraction purity.

Chemical	Provenance	CAS number	Purification method	Mass fraction purity	Analysis method
1-Ethyl-3-methylimidazolium ethyl sulfate	Io-Li-Tec, Germany	342573-75-5	NA	0.99	NA
2-Ethoxyethanol	Sigma-Aldrich	110-80-5	Distillation	0.99	Gas liquid chromatography

Table 2
Comparison of experimental values of density, ρ, speed of sound, u, refractive index, n_D, and specific heat, C_p, of pure liquids at atmospheric pressure with the corresponding literature values at different temperatures.

Liquid	Temp/	ρ/(kg m^{-3})		u/(ms^{-1})		n_D		C_p/(J K^{-1} mol^{-1})
	(K)	Expt.	Litt.	Expt.	Litt.	Expt.	Litt.	Litt.
	298.15	1236.379	1236.24 [42]	1680.78	1679.00 [38]	1.477556	1.4789 [44]	394.4 [39]
	308.15	1229.493	1229.42 [42]	1656.42	–	1.474977	1.4763 [44]	399.3 [39]
	318.15	1222.779	1222.66 [42]	1632.4	–	1.472283	–	404.9 [39]
[Emim][EtSO$_4$]	328.15	1216.157	1215.96 [42]	1608.9	1605.00 [38]	1.469658	–	410.0 [45]
	298.15	925.927	925.999 [36]	1302.75	1303.06 [36]	1.405695	1.4058 [46]	209.82 [47]
	308.15	916.881	916.868 [36]	1268.58	1267.68 [36]	1.401527		214.01 [47]
	318.15	907.675	907.588 [36]	1233.26	1232.39 [36]	1.397264		218.20 [47]
2-ethoxyethanol	328.15	898.047	–	1198.83	–	1.392958		222.40 [47]

3. Theory

The experimentally measured values of ρ, u and n_D were used to calculate the values of thermodynamic and acoustical parameters such as molar volume (V_m), intermolecular free length (L_f), isentropic compressibility (κ_S) and isobaric thermal expansion coefficient (α_P). An attempt has been made to calculate thermodynamic parameters such as isothermal compressibility (κ_T), internal pressure (π_i) and free volume (V_f) assuming the specific heats of the binary mixtures as ideal. The experimentally measured values and the derived parameter values were shown in Table 3. The excess/deviation parameters for the above parameters including deviations in refractive index ($\Delta_\phi n_D$), $\left(\frac{\partial V_m^E}{\partial T}\right)_P$ and $\left(\frac{\partial H_m^E}{\partial P}\right)_{T=298.15K}$ were also calculated by using the following equations:

$$V_m = \frac{M_{eff}}{\rho} \tag{1}$$

where M_{eff} is given by $M_{eff} = (x_1M_1 + x_2M_2)$, where M_1 and M_2 are the molar masses of pure components and ρ is the density of the medium. x_1 and x_2 are the mole fractions of IL and 2-ethoxyethanol respectively.

The speed of sound (u) and the density of the medium (ρ) using the Newton and Laplace equation give free length as:

$$L_f = \frac{K}{\sqrt{\rho u^2}} \tag{2}$$

where, K is the temperature dependent constant which is equal to $K = (93.875 + 0.375\,T) \times 10^{-8}$.

The excess molar volumes are given by

$$V_m^E = \frac{x_1M_1 + x_2M_2}{\rho} - \left(\frac{x_1M_1}{\rho_1} + \frac{x_2M_2}{\rho_2}\right) \tag{3}$$

where, M_1 & M_2 are the molecular weights, x_1 & x_2 are the mole fractions of IL and 2-ethoxyethanol respectively, while ρ_1, ρ_2 & ρ are the densities of IL, 2-ethoxyethanol and the mixture respectively.

The excess intermolecular free length at a given mole fraction is the difference between mean free length and the sum of the fractional contributions of the two liquids and it is given by

$$L_f^E = L_f - L_f^{id} = L_f - (x_1L_{f,1} + x_2L_{f,2}) \tag{4}$$

where, $L_{f,1}$ and $L_{f,2}$ are the intermolecular free lengths, while x_1 and x_2 are the mole fractions of IL and 2-ethoxyethanol respectively.

The isentropic compressibility,κ_S, is computed directly from the measured values of speed of sound and density using the Newton–Laplace equation

$$\kappa_s = -\frac{1}{V_m}\left(\frac{\partial V_m}{\partial P}\right)_s = \left(\frac{1}{\rho u^2}\right) = \left(\frac{V_m}{Mu^2}\right). \tag{5}$$

Excess isentropic compressibility is given by

$$\kappa_s^E = \kappa_s - \kappa_s^{id} \tag{6}$$

where, κ_S, is the isentropic compressibility and κ_S^{id}, is the isentropic compressibility of the ideal mixture, which is calculated in the manner as suggested by Benson and Kiyohara [49].

$$\kappa_S^{id} = \sum_{i=1}^{2} \phi_i \left[\kappa_{S,i} + \frac{TV_i\alpha_i^2}{C_{p,i}}\right] - \left\{T\frac{\left(\sum_{i=1}^{2} x_iV_i\right)\left(\sum_{i=1}^{2} \phi_i\alpha_i\right)^2}{\left(\sum_{i=1}^{2} x_iC_{p,i}\right)}\right\} \tag{7}$$

where, ϕ_i, is the volume fraction of the i^{th} component and is given by, $\phi_i = \frac{x_iV_i}{\sum_{i=1}^{2} x_iV_i}$, T is the temperature, $\kappa_{S,i}$, is the isentropic compressibility,V_i, is the molar volume, α_i, is the isobaric thermal expansion coefficient, and $C_{P,i}$, heat capacity of the i^{th} component.

The excess speed of sound, u^E is estimated in binary and ternary mixtures using the following expressions [50].

$$u^E = u - u^{id} = u - \left(\rho^{id}k_S^{id}\right)^{-1/2} \tag{8}$$

where $\rho^{id} = \sum_{i=1}^{2} \phi_i\rho_i$.

Isobaric thermal expansion coefficient, α_p, of the pure components is calculated from the measured densities by the relation,

$$\alpha_p = \frac{1}{V_m}\left(\frac{\partial V_m}{\partial T}\right)_p = -\frac{1}{\rho}\left(\frac{\partial \rho}{\partial T}\right)_p = -\left(\frac{\partial \ln\rho}{\partial T}\right). \tag{9}$$

Excess isobaric thermal expansion coefficient, α_P^E, is calculated from the following equation

$$\alpha_P^E = \alpha_P - \alpha_P^{id} = \frac{\left(\frac{\partial V_m^E}{\partial T}\right)_P - V_m^E\alpha_P^{id}}{V_m^{id} + V_m^E} \tag{10}$$

where, $\alpha_P^{id} = \sum_{i=1}^{2} \phi_i\alpha_{P,i}^*$ and ϕ_i, are the volume fractions of the i^{th} component, $\phi_i = \frac{x_iV_i}{\sum_{i=1}^{2} x_iV_i}$.

Table 3
Experimental density (ρ), speed of sound (u), refractive index (n_D), molar volume (V_m), isentropic compressibility (κ_s), isothermal compressibility (κ_T), free length (L_f), internal pressure (π_i), free volume (V_f) and isobaric thermal expansion coefficient (α_p) with mole fraction (x_1) of 1-ethyl-3-methylimidazolium ethylsulfate in the binary liquid mixture of {1-ethyl-3-methylimidazolium ethylsulfate + 2-ethoxyethanol} from T/K = 298.15 to 328.15 at pressure P = 0.1 MPa.

x_1	ρ/	u/	n_D	V_m/	κ_s/	κ_T/	L_f/	π_i/	V_f/	α_p/
	(kg m^{-3})	(ms^{-1})		(10^{-6} m3 mol^{-1})	(10^{-10} Pa^{-1})	(10^{-10} Pa^{-1})	(10^{-1} 1 m)	(10^{7} Pa)	(10^{-7} m^3 mol^{-1})	(10^{-4} K^{-1})
298.15 K										
0.00000	925.927	1302.75	1.405695	97.3295	6.3636	7.7542	5.1885	38.5554	64.2924	10.0274
0.04876	956.614	1333.20	1.412714	101.6578	5.8813	7.0746	4.9881	39.1168	63.3697	9.2817
0.09058	980.355	1356.80	1.418446	105.4313	5.5410	6.6125	4.8416	39.6225	62.5608	8.7877
0.13425	1002.951	1379.57	1.423933	109.4204	5.2388	6.2103	4.7077	40.1275	61.7736	8.3584
0.17272	1021.268	1398.51	1.428383	112.9640	5.0064	5.9063	4.6021	40.5661	61.1057	8.0361
0.25898	1057.897	1438.59	1.437206	120.9712	4.5675	5.3459	4.3958	41.5850	59.6084	7.4563
0.34705	1089.863	1476.34	1.444821	129.2349	4.2097	4.9024	4.2201	42.6727	58.0891	7.0165
0.44890	1121.439	1516.77	1.452234	138.8713	3.8760	4.4985	4.0494	43.9650	56.3816	6.6335
0.54838	1148.005	1553.43	1.458358	148.3240	3.6097	4.1808	3.9078	45.1982	54.8433	6.3380
0.64522	1170.791	1586.59	1.463506	157.5275	3.3931	3.9235	3.7887	46.3163	53.5193	6.0950
0.76737	1196.221	1624.58	1.469118	169.1046	3.1674	3.6557	3.6606	47.5822	52.0955	5.8342
0.81543	1205.366	1638.16	1.471098	173.6497	3.0915	3.5660	3.6164	48.0485	51.5899	5.7468
0.87976	1216.901	1654.88	1.473562	179.7307	3.0006	3.4588	3.5629	48.6289	50.9742	5.6414
0.94121	1227.187	1669.07	1.475716	185.5436	2.9251	3.3693	3.5177	49.1065	50.4785	5.5493
1.00000	1236.379	1680.78	1.477556	191.1145	2.8630	3.2921	3.4802	49.3557	50.2236	5.4498
308.15 K										
0.00000	916.881	1268.58	1.401527	98.2897	6.7772	8.2284	5.4521	37.9223	67.5581	10.1263
0.04876	947.897	1300.23	1.408714	102.5926	6.2402	7.4838	5.2317	38.5693	66.4248	9.3671
0.09058	971.879	1324.70	1.414592	106.3508	5.8634	6.9792	5.0713	39.1382	65.4593	8.8643
0.13425	994.689	1348.24	1.420210	110.3293	5.5307	6.5415	4.9253	39.7005	64.5321	8.4278
0.17272	1013.166	1367.78	1.424760	113.8673	5.2758	6.2116	4.8104	40.1847	63.7546	8.1004
0.25898	1050.075	1408.95	1.433767	121.8723	4.7972	5.6061	4.5871	41.2906	62.0470	7.5118
0.34705	1082.247	1447.58	1.441532	130.1443	4.4095	5.1289	4.3978	42.4525	60.3488	7.0659
0.44890	1114.008	1488.90	1.449090	139.7977	4.0493	4.6957	4.2144	43.8219	58.4630	6.6777
0.54838	1140.725	1526.37	1.455344	149.2706	3.7627	4.3556	4.0625	45.1258	56.7737	6.3784
0.64522	1163.648	1560.31	1.460613	158.4945	3.5299	4.0805	3.9348	46.3109	55.3208	6.1324
0.76737	1189.238	1599.25	1.466367	170.0976	3.2877	3.7945	3.7974	47.6573	53.7580	5.8685
0.81543	1198.440	1613.17	1.468396	174.6532	3.2064	3.6989	3.7502	48.1525	53.2051	5.7801
0.87976	1210.033	1630.26	1.470911	180.7509	3.1095	3.5850	3.6931	48.7660	52.5357	5.6734
0.94121	1220.336	1644.67	1.473094	186.5852	3.0294	3.4904	3.6452	49.2665	52.0021	5.5804
1.00000	1229.493	1656.42	1.474977	192.1849	2.9644	3.4098	3.6059	49.5263	51.7293	5.4803
318.15 K										
0.00000	907.675	1233.26	1.397264	99.2866	7.2437	8.7584	5.7376	37.1569	71.1874	10.2290
0.04876	939.063	1266.36	1.404629	103.5577	6.6403	7.9362	5.4934	37.9045	69.7832	9.4552
0.09058	963.309	1291.91	1.410627	107.2969	6.2197	7.3810	5.3166	38.5487	68.6171	8.9432
0.13425	986.351	1316.44	1.416359	111.2619	5.8501	6.9012	5.1562	39.1810	67.5098	8.4990
0.17272	1005.004	1336.74	1.421001	114.7921	5.5685	6.5409	5.0306	39.7200	66.5936	8.1662
0.25898	1042.232	1379.32	1.430189	122.7895	5.0432	5.8827	4.7874	40.9316	64.6225	7.5684
0.34705	1074.645	1419.09	1.438111	131.0650	4.6208	5.3669	4.5825	42.1831	62.7052	7.1159
0.44890	1106.614	1461.44	1.445829	140.7317	4.2310	4.9009	4.3850	43.6388	60.6134	6.7223
0.54838	1133.494	1499.75	1.452220	150.2229	3.9223	4.5366	4.2220	45.0168	58.7581	6.4191
0.64522	1156.557	1534.43	1.457612	159.4662	3.6723	4.2426	4.0852	46.2686	57.1683	6.1700
0.76737	1182.304	1574.18	1.463500	171.0951	3.4132	3.9379	3.9385	47.6902	55.4642	5.9029
0.81543	1191.558	1588.38	1.465573	175.6620	3.3264	3.8363	3.8881	48.2120	54.8639	5.8134
0.87976	1203.213	1605.82	1.468139	181.7754	3.2230	3.7153	3.8272	48.8585	54.1379	5.7056
0.94121	1213.571	1620.49	1.470358	187.6253	3.1379	3.6151	3.7763	49.3850	53.5608	5.6115
1.00000	1222.779	1632.40	1.472283	193.2402	3.0690	3.5301	3.7346	49.6629	53.2611	5.5104
328.15 K										
0.00000	898.047	1198.83	1.392958	100.3511	7.7479	9.3306	6.0383	36.3603	75.0335	10.3387
0.04876	929.962	1232.92	1.400609	104.5712	7.0740	8.4250	5.7697	37.1881	73.3632	9.5477
0.09058	954.495	1259.30	1.406735	108.2877	6.6064	7.8157	5.5758	37.8956	71.9935	9.0257
0.13425	977.787	1284.67	1.412581	112.2364	6.1969	7.2903	5.4002	38.5908	70.6967	8.5735
0.17272	996.632	1305.68	1.417310	115.7563	5.8856	6.8965	5.2628	39.1825	69.6289	8.2348
0.25898	1034.218	1349.73	1.426662	123.7409	5.3076	6.1792	4.9977	40.5036	67.3580	7.6270
0.34705	1066.907	1390.81	1.434722	132.0155	4.8455	5.6196	4.7752	41.8539	65.1848	7.1675
0.44890	1099.107	1434.40	1.442584	141.6929	4.4220	5.1167	4.5618	43.4071	62.8524	6.7683
0.54838	1126.162	1473.66	1.449113	151.2009	4.0889	4.7256	4.3866	44.8649	60.8101	6.4609
0.64522	1149.368	1509.04	1.454639	160.4637	3.8207	4.4117	4.2403	46.1813	59.0767	6.2086
0.76737	1175.269	1549.45	1.460686	172.1193	3.5441	4.0877	4.0839	47.6699	57.2319	5.9382
0.81543	1184.570	1563.87	1.462811	176.6982	3.4517	3.9800	4.0303	48.2149	56.5849	5.8477
0.87976	1196.291	1581.61	1.465431	182.8272	3.3417	3.8516	3.9656	48.8918	55.8016	5.7386
0.94121	1206.742	1596.60	1.467675	188.6871	3.2508	3.7451	3.9113	49.4477	55.1742	5.6433
1.00000	1216.157	1608.90	1.469658	194.2923	3.1765	3.6539	3.8663	49.7578	54.8304	5.5404

Standard uncertainties U are: U(x_1) = 0.0001, U(ρ) = 0.001 kg m^{-3}, U(u) = 0.01 ms^{-1}, U(n_D) = 0.00005 and U(T) = 0.01 K.
Combined uncertainties (confidence level, 95%).: U (V_m) = $\pm 0.016 \times 10^{-6}$ m^3 mol^{-1}, U(κ_s) = $\pm 0.029 \times 10^{-10}$ Pa^{-1}, U (κ_T) = $\pm 0.048 \times 10^{-10}$ Pa^{-1}, U (L_f) = $\pm 0.008 \times 10^{-11}$ m, U (π_i) = $\pm 0.05 \times 10^{7}$ Pa, U (V_f) = $\pm 0.075 \times 10^{-7}$ m^3 mol^{-1}, U (α_p) = $\pm 0.04 \times 10^{-4}$ K^{-1}. All the experiments were carried out at atmospheric pressure.

The dependence of the excess molar enthalpy of mixing with pressure at fixed temperature $\left(\frac{\partial H_m^E}{\partial P}\right)_T$ can be derived indirectly from accurate measurement of V_m^E, as a function of the temperature and composition by application of the following exact thermodynamic expression

$$\left(\frac{\partial H_m^E}{\partial P}\right)_T = V_m^E - T\left(\frac{\partial V_m^E}{\partial T}\right)_P. \tag{11}$$

A liquid undergoing a small, isothermal volume expansion does work against the cohesive forces causing a change in the internal energy, U.

$$\pi_i = \left(\frac{\partial U}{\partial V}\right)_T \tag{12}$$

where, U is the internal energy, V the volume and T the temperature.

From the thermodynamic equation of state,

$$\left(\frac{\partial U}{\partial V}\right)_T = T\left(\frac{\partial P}{\partial T}\right)_V - P \tag{13}$$

where, P is the external pressure and $\left(\frac{\partial P}{\partial T}\right)_V = \frac{\alpha_p}{\kappa_T}$, where,$\alpha_p$ and κ_T are the isobaric thermal expansion coefficient and isothermal compressibility of the mixture. Therefore Eq. (13) can be written as

$$\pi_i = T\frac{\alpha_p}{\kappa_T} - P. \tag{14}$$

At low external pressures (i.e., 1 atm.), the second term of Eq. (16) can be neglected [51] without significant error because $P \ll T\frac{\alpha_p}{\kappa_T}$

$$\therefore \pi_i = \frac{\alpha_p T}{\kappa_T}. \tag{15}$$

Thus, apart from the direct method [52–55], the internal pressure can be calculated from direct or indirect measurements of the isothermal compressibility coefficient [56]. The well-known acoustic method is the convenient and well-established method for the determination of κ_T [57,58] (and, as a result, P_{int}).

$$\kappa_T - \frac{1}{U^2\rho} = \frac{\alpha^2 T V_m}{C_p} \Rightarrow \kappa_T = \kappa_S + \frac{\alpha^2 T V_m}{C_p} \Rightarrow \tag{16}$$

where, C_P is the heat capacity of the mixture. The α_P values for the mixtures were calculated from temperature dependence of density data and C_P values for the mixtures have been calculated by using the relation.

$$C_p^{id} = x_1 C_{p,1} + x_2 C_{p,2}$$

The excess internal pressure [59], π_i^E, is given by

$$\pi_i^E = \left(\frac{\alpha T}{\kappa_T} - \frac{\sum \phi_i \alpha_i T}{\sum \phi_i \kappa_{Ti}}\right). \tag{17}$$

The excess isothermal compressibility, κ_T^E is estimated in binary and ternary mixtures using the following expressions:

$$\kappa_T^E = \kappa_T - \left(x_1\kappa_{T,1} + x_2\kappa_{T,2}\right). \tag{18}$$

The free volumes, V_f of the mixtures are calculated from the relation

$$V_f = \frac{RT}{P + \pi_i}. \tag{19}$$

Since P is very small compared to π_i, it is neglected in Eq. (19).

$$V_f = \frac{RT}{\pi_i} \tag{20}$$

The excess free volume, V_f^E, at a given mole fraction is the difference between free volume and the sum of the fractional contributions of the two liquids given by

$$V_f^E = V_f - \sum_{i=1}^{2} x_i V_{fi}. \tag{21}$$

If the difference between the refractive indices of the two components is small then deviation in refractive index of binary mixtures containing ILs is given by

$$\begin{aligned} \Delta_\phi n_D &= n_D - n_D^{id} \\ n_D^{id} &= \phi_1 n_{D,1} + \phi_2 n_{D,2} \end{aligned} \tag{22}$$

The excess/deviation properties have been fitted to a Redlich–Kister type polynomial equation given by

$$Y^E = x_1 x_2 \sum_{i=o}^{j} A_i (x_2 - x_1)^i \tag{23}$$

where $Y^E = V_m^E$, ,L_f^E, u^E, κ_T^E,π_i^E,V_f^E,α_P^E and $\Delta_\phi n_D$. x_1 and x_2 are the mole fractions of ionic liquid and 2-ethoxyethanol respectively. Further, A_i is the adjustable parameter of the function; and is determined using the least square method. In the present investigation '*i*' values have been taken from 0 to 4. The corresponding standard deviations $\sigma(Y^E)$ have been calculated using the following expressions

$$\sigma\left(Y^E\right) = \left[\frac{\sum\left(Y_{exp}^E - Y_{cal}^E\right)}{(m-n)}\right]^{1/2} \tag{24}$$

where 'm' is the total number of experimental points and 'n' is the number of coefficients in Eq. (23). The calculated values of the coefficients A_i along with the standard deviations $\sigma(Y^E)$ and correlation coefficient (R^2) are given in Table 4.

4. Results and discussion

In the present study, the excess and deviation parameters are calculated. The variations as observed in these excess/deviation parameters, indicate the strength of interactions that exist between the component molecules of the binary mixture under study and their further dependence on the composition, molecular size, shape and temperature. The effects which influence these thermodynamic functions may be the resultant contribution from several opposing effects, namely chemical, structural, and physical [60]. The chemical or specific interactions include the formation of hydrogen bonding between component molecules, charge-transfer complexes. The structural contributions arise from several effects such as interstitial accommodation and geometrical fitting of one component into another due to considerable difference in the molar volume between component molecules. The physical interactions or non-specific interactions are due to dispersion type of forces.

Excess molar volumes V_m^E for binary mixture of [Emim][$EtSO_4$] + 2-ethoxyethanol as a function of composition from T = 298.15 K to T = 328.15 K are shown in Fig. 1. Excess molar volumes are found to be negative in the entire composition at all temperatures. This indicates

Table 4
Redlich–Kister coefficients of deviation/excess properties along with corresponding standard deviations (σ) and correlation coefficient (R^2) for the systems at different temperatures.

	T/K	A_0	A_1	A_2	A_3	A_4	σ	R^2
V_m^E / (10^{-6} m^3 mol^{-1})	298.15	−1.9954	−2.3911	−0.9105	0.2255	−0.6293	0.0049	0.9997
	308.15	−2.3105	−2.5833	−1.1348	0.2896	−0.6930	0.0048	0.9998
	318.15	−2.6431	−2.8234	−1.3051	0.2331	−0.6982	0.0052	0.9998
	328.15	−3.0008	−3.1312	−1.4129	−0.1404	−0.6720	0.0077	0.9979
κ_s^E / (10^{-10} Pa^{-1})	298.15	−1.4147	−0.9906	−0.7211	−0.6741	−0.5393	0.0021	0.9999
	308.15	−1.6427	−1.1682	−0.8668	−0.7931	−0.6256	0.0023	0.9999
	318.15	−1.9326	−1.4050	−1.0384	−0.9429	−0.7308	0.0027	0.9999
	328.15	−2.2603	−1.6621	−1.1826	−1.0940	−0.8403	0.0031	0.9998
u^E / (ms^{-1})	298.15	261.34	45.63	52.20	28.75	29.34	0.13	0.99
	308.15	283.89	48.31	59.11	28.56	29.81	0.13	0.99
	318.15	312.07	52.70	64.12	28.67	29.99	0.13	0.99
	328.15	340.78	53.63	62.05	28.96	29.68	0.13	0.99
L_f^E / (10^{-11} m)	298.15	0.0000	−1.4429	−0.5636	−0.3212	−0.2281	−0.1827	0.9999
	308.15	0.0000	−1.5835	−0.6317	−0.3746	−0.2590	−0.2054	0.9999
	318.15	0.0000	−1.7535	−0.7207	−0.4324	−0.2973	−0.2313	0.9999
	328.15	0.0000	−1.9380	−0.8120	−0.4706	−0.3359	−0.2574	0.9999
$\Delta_{\varnothing} n_D$	298.15	0.008719	0.006371	0.003500	−0.004446	−0.004200	0.000032	0.998954
	308.15	0.008864	0.006598	0.004520	−0.004427	−0.005083	0.000034	0.998887
	318.15	0.009003	0.006572	0.004860	−0.004113	−0.005105	0.000031	0.999100
	328.15	0.009084	0.006575	0.005752	−0.002739	−0.004486	0.000019	0.999665
κ_T^E/(10^{-10} Pa^{-1})	298.15	−4.7880	−2.4865	−1.4678	−1.2818	−0.9398	0.0042	0.9999
	308.15	−5.2321	−2.7442	−1.6514	−1.4336	−1.0516	0.0046	0.9999
	318.15	−5.7650	−3.0691	−1.8630	−1.6204	−1.1858	0.0051	0.9999
	328.15	−6.3535	−3.4196	−2.0469	−1.8175	−1.3341	0.0057	0.9999
π_i^E / (10^7 Pa)	298.15	4.5657	−3.0173	−0.7874	−0.2014	3.2140	0.0156	0.9999
	308.15	5.4891	−2.8961	−0.3971	−0.2160	3.2585	0.0156	0.9999
	318.15	6.7000	−2.6758	−0.1057	−0.2065	3.2856	0.0156	0.9999
	328.15	7.9361	−2.6158	−0.1884	−0.1501	3.2927	0.0152	0.9999
V_f^E / (10^{-7} m^3 mol^{-1})	298.15	−6.7430	2.4332	1.5593	−0.0941	−3.8710	0.0175	0.9999
	308.15	−8.2798	1.9360	1.0229	−0.2742	−4.1201	0.0180	0.9999
	318.15	−10.3575	1.0718	0.4740	−0.5214	−4.3867	0.0184	0.9999
	328.15	−12.6392	0.2641	0.4295	−0.7071	−4.6377	0.0183	0.9999
α_p^E(10^{-4} K^{-1})	298.15	−2.0870	−2.1353	−1.6324	−1.3715	−0.5871	0.0072	0.9994
	308.15	−2.1337	−2.1840	−1.6717	−1.3938	−0.6036	0.0074	0.9994
	318.15	−2.1811	−2.2279	−1.7108	−1.4414	−0.6308	0.0073	0.9994
	328.15	−2.2353	−2.2871	−1.7475	−1.4880	−0.6637	0.0078	0.9994

the presence of strong interactions between the liquids in study like formation of H-bonding and fitting of smaller into voids created by the bigger molecules [39]. Generally, imidazolium ionic liquids are polar solvents under favorable conditions that can form hydrogen bond as these act as donors and acceptors of protons [61]. Hence, we can assume that the hydrogen bonds between the ionic liquid [Emim][$EtSO_4$] and 2-ethoxyethanol are responsible to make a remarkable contraction in the volume of the mixture. Further, favorable fitting of smaller 2-ethoxyethanol molecules (at T = 298.15 K, V_m = 97.3295 × 10^{-6} m^3 mol^{-1}) into the voids created by larger IL molecules (at T = 298.15 K, V_m = 191.1145 × 10^{-6} m^3 mol^{-1}) also contribute to strong interaction. The same type of trend can be observed at other investigated temperatures also. The values of V_m^E become more negative with the increase in temperature for the system under study. This is due to the fact that, more favorable fitting of smaller 2-ethoxyethanol molecules into the voids created by larger IL molecules occurs, thereby, reducing the volume of the mixture to a larger extent, resulting in more negative V_m^E values with the increase in temperature. The order of strength of interaction thus follows: (328.15 > 318.15 > 308.15 > 298.15) K.

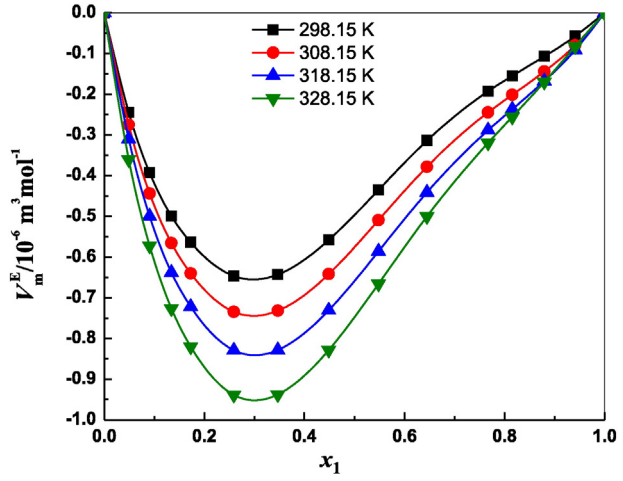

Fig. 1. Plots of excess molar volume (V_m^E) against mole fraction of [Emim][$EtSO_4$] with 2-ethoxyethanol at different temperatures.

The existing molecular interactions in the system are well reflected on the properties of partial molar volumes. Partial molar volume is the contribution that a component of a mixture makes to the overall volume of the solution and hence, it is a function of mixture composition. The partial molar volumes $\overline{V}_{m,1}$ of component **1**([Emim][$EtSO_4$]) and $\overline{V}_{m,2}$ of component **2** (2-ethoxyethanol) in the mixtures over the entire composition range have been calculated by using the following relations.

$$\overline{V}_{m,1} = V_m^E + V_1^* + x_2\left(\frac{\partial V_m^E}{\partial x_1}\right)_{T,P} \tag{25}$$

$$\overline{V}_{m,2} = V_m^E + V_2^* - x_1\left(\frac{\partial V_m^E}{\partial x_1}\right)_{T,P} \tag{26}$$

where V_1^* and V_2^* are the molar volumes of pure components of [Emim][$EtSO_4$] and 2-ethoxyethanol respectively. The derivatives in

the above equations are obtained by differentiating Redlich–Kister Eq. (23) which leads to the following equations for $\overline{V}_{m,1}$ and $\overline{V}_{m,2}$.

$$\overline{V}_{m,1} = V_1^* + x_2^2\sum_{i=0}^{4} A_i(x_2-x_1)^i - 2x_1x_2^2\sum_{i=1}^{4} A_i(i)(x_2-x_1)^{i-1} \quad (27)$$

$$\overline{V}_{m,2} = V_2^* + x_1^2\sum_{i=0}^{4} A_i(x_2-x_1)^i + 2x_2x_1^2\sum_{i=1}^{4} A_i(i)(x_2-x_1)^{i-1} \quad (28)$$

Using the above equations $\overline{V}^E_{m,1}$ and $\overline{V}^E_{m,2}$ have been calculated using,

$$\overline{V}^E_{m,1} = \overline{V}_{m,1} - V_1^* \quad (29)$$

$$\overline{V}^E_{m,2} = \overline{V}_{m,2} - V_2^*. \quad (30)$$

The values of $\overline{V}_{m,1}$ and $\overline{V}_{m,2}$ are presented in Table 5 for the system. From this table, it was observed that the values of $\overline{V}_{m,1}$ and $\overline{V}_{m,2}$ for both the components in the mixtures are almost lower than their individual molar volumes in the pure state, which indicates that contraction of volume takes place on mixing [Emim][$EtSO_4$]with 2-ethoxyethanol at all the temperatures. Figs. 2 and 3 represent the disparity of excess partial molar volumes of $\overline{V}^E_{m,1}$ ([Emim][$EtSO_4$]) and $\overline{V}^E_{m,2}$ (2-ethoxyethanol) respectively in the binary mixture at T = (298.15, 308.15, 313.15 and 318.15) K. Inspection of these figures does not only reveals the existence of strong forces between the unlike molecules but also supports the deductions drawn from excess molar volume. The partial properties at infinite dilution are of interest since; these values of the partial molar volume at infinite dilution provide information about solute–solvent interaction, independent of the composition effect. The partial molar volumes and excess partial molar volumes of [Emim][EtSO4] at infinite dilution, $\overline{V}^{\infty}_{m,1}$ and $\overline{V}^{E,\infty}_{m,1}$ have been given by

$$\overline{V}^{\infty}_{m,1} = A_0 + A_1 + A_2 + A_3 + \ldots\ldots = \overline{V}^{\infty}_{m,1} - \overline{V}^*_{m,1}. \quad (31)$$

The pertinent data of $\overline{V}^{\infty}_{m,1}$ and $\overline{V}^{E,\infty}_{m,1}$ have been presented in Table 6 at T = (298.15/308.15/313.15/318.15) K. From this table, the values of $\overline{V}^{\infty}_{m,1}$ are found to be negative and become more negative with the increase of temperature. Hence, it can be concluded that strong interactions increase among the unlike molecules of the mixtures with increase in temperature. This argument supports the existing strong

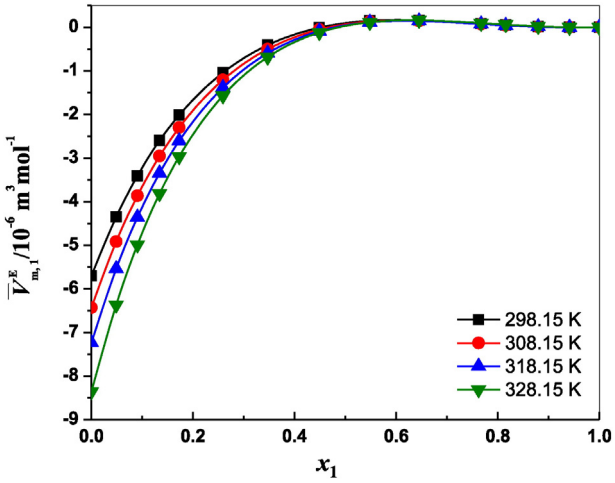

Fig. 2. Plots of excess partial molar volume ($\overline{V}^E_{m,1}$) against mole fraction of [Emim][$EtSO_4$] with 2-ethoxyethanol at different temperatures.

molecular interactions as noticed in the case of $\overline{V}^E_m$ values in the binary system which are well reproduced from the evaluated properties of partial molar volumes as well as at all investigated temperatures.

Isentropic compressibility (κ_s) values are presented in Table 3 and their excess values (κ^E_s) are calculated by using Eqs. (5), (6) and (7) as suggested by Benson and Kiyohara [49]. From Table 3 it can be visualized that the isentropic compressibility decreases with the increase in concentration of [Emim][$EtSO_4$] which may be attributed to the aggregation of solvent molecules around the ions supporting solute–solvent interaction. This suggests that when the IL [Emim][$EtSO_4$] is added to solvent 2-ethoxyethanol, the ions of the IL attract certain solvent molecules towards itself by wrenching the molecule species from the bulk of the solvent. Hence, less number of solvent molecules will be made available for the next incoming species, known as compression. In Fig. 4, the $_s{}^E$values for [Emim][$EtSO_4$] + 2-ethoxyethanol are negative in the whole composition range at all investigated temperatures. The negative^E_s values are attributed to the strong attractive interactions between the molecules of the components [62]. This supports the inference drawn from V^E_m.

Figs. 5 and 6 represent L^E_f & κ^E_T respectively which show the trend similar to that of ^E_s at all investigated temperatures. The negative values

Table 5
Partial molar volumes of component-1 ($\overline{V}_{m,1}$) (1-ethyl-3-methylimidazolium ethylsulfate) and component-2 ($\overline{V}_{m,2}$) (2-ethoxyethanol) with mole fraction (x_1) of 1-ethyl-3-methylimidazolium ethylsulfate in the binary liquid mixture from T/K = 298.15 to 328.15 at pressure P = 0.1 MPa.

x_1	298.15 K		308.15 K		318.15 K		328.15 K	
	$\overline{V}_{m,1}$	$\overline{V}_{m,2}$	$\overline{V}_{m,1}$	$\overline{V}_{m,2}$	$\overline{V}_{m,1}$	$\overline{V}_{m,2}$	$\overline{V}_{m,1}$	$\overline{V}_{m,2}$
	/10^{-6} m^3 mol^{-1}		/10^{-6} m^3 mol^{-1}		/10^{-6} m^3 mol^{-1}		/10^{-6} m^3 mol^{-1}	
0.00000	185.4138	97.3295	185.7556	98.2897	186.0034	99.2866	185.9351	100.3511
0.04876	186.7658	97.3015	187.2685	98.2584	187.6986	99.2515	187.9246	100.3105
0.09058	187.7076	97.2410	188.3236	98.1907	188.8818	99.1758	189.3049	100.2237
0.13425	188.5145	97.1522	189.2284	98.0914	189.8964	99.0647	190.4806	100.0971
0.17272	189.1001	97.0587	189.8852	97.9868	190.6329	98.9478	191.3280	99.9650
0.25898	190.0750	96.8205	190.9786	97.7208	191.8574	98.6514	192.7219	99.6334
0.34705	190.7051	96.5715	191.6843	97.4437	192.6463	98.3430	193.6081	99.2916
0.44890	191.1084	96.3249	192.1354	97.1694	193.1515	98.0368	194.1730	98.9509
0.54838	191.2675	96.1716	192.3152	96.9960	193.3569	97.8384	194.4094	98.7223
0.64522	191.2797	96.1337	192.3343	96.9422	193.3865	97.7662	194.4551	98.6279
0.76737	191.2018	96.2258	192.2600	97.0028	193.3157	97.8101	194.3890	98.6787
0.81543	191.1674	96.2758	192.2278	97.0285	193.2836	97.8306	194.3540	98.7260
0.87976	191.1328	96.3049	192.1971	97.0044	193.2526	97.8000	194.3161	98.7696
0.94121	191.1170	96.2256	192.1853	96.8404	193.2407	97.6298	194.2966	98.7308
1.00000	191.1145	95.9599	192.1849	96.4478	193.2402	97.2305	194.2923	98.5370

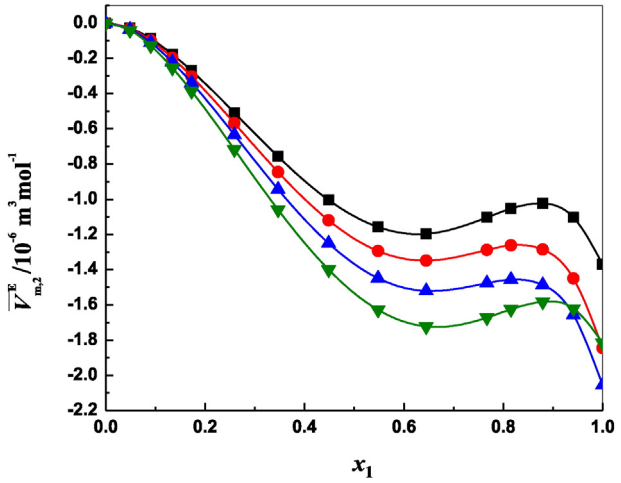

Fig. 3. Plots of excess partial molar volume ($\overline{V}^{E}_{m,2}$) against mole fraction of [Emim][$EtSO_4$] with 2-ethoxyethanol at different temperatures.

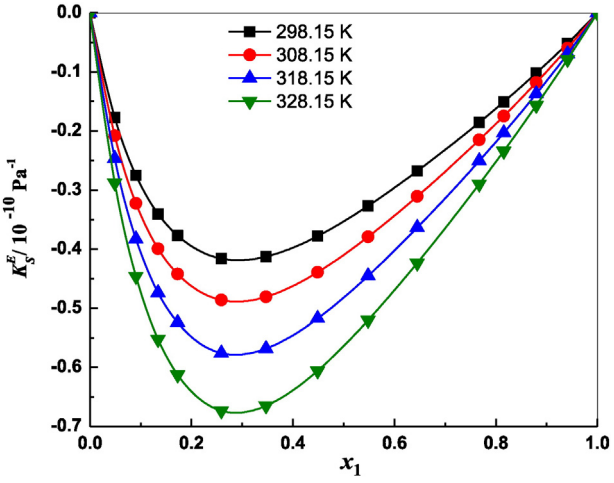

Fig. 4. Plots of excess isentropic compressibility (κ_S^E) against mole fraction of [Emim][$EtSO_4$] with 2-ethoxyethanol at different temperatures.

of L_f^E and κ_T^E attributed to closer approach of unlike molecules indicate stronger interaction between components of mixtures at all temperatures [62,63].

Excess speed of sound values are calculated from Eq. (8) as proposed by Douheret et al. [50]. Fig. 7 shows that the u^E values are positive for the system over the entire range of composition at all the studied temperatures. Excess positive values indicate the increasing strength of interaction between component molecules of binary liquid mixtures. In general, strong interactions among the components of a mixture lead to the formation of molecular aggregates and more compact structures; then sound will travel faster through the mixture by means of longitudinal waves resulting in the ultrasonic speed deviations with respect to a linear behavior will be positive, if the structure-breaking factor in the mixture predominates resulting in expansion, then the speed of sound through the mixture will be slower resulting in negative deviation in the speed of sound [64]. According to Ali et al. [65], more positive values mean much more strong interactions between the molecules.

The refractive indices (n_D) for the binary mixtures at the studied temperatures over the whole composition range were calculated from Eq. (22) and are given in Table 3. Refractive index increases as the concentration of the ILs in the mixture increases. For the fixed concentration of the IL, as the temperature increases, n_D decreases which may be due to the non-availability of the free volume in the mixture as compared to the ideal mixtures. It is well supported by comparing $\Delta_\phi n_D$ with V_m^E. The values of $\Delta_\phi n_D$ are positive over the studied range of composition for the binary mixtures (Fig. 8). As the mole fraction of the ILs increases V_m^E becomes more negative as the free volume available decreases in the mixtures and the speed of light travels with lesser velocity than that in the ideal mixtures [66]. Thus it further supports the presence of strong interactions between component molecules in study.

Generally, the cohesive forces (attraction forces) or dispersive forces between the molecules of a mixture cannot be easily assessed by any theory. However, they can be accurately estimated via the evaluation of thermodynamic parameters such as internal pressure (π_i^E) that is inversely related to the free volume (V_f^E). Figs. 9 and 10 show that the values of π_i^E are positive and V_f^E is negative over the entire mole fraction range and at all temperatures investigated for the binary mixture and also indicates the presence of strong interactions between [Emim][EtSO4] and 2-ethoxyethanol. The strong attractions may be attributed to geometrical fitting due to a large difference in the size of the constituent molecules and also to the formation of hydrogen bonds, formation of charge transfer complexes and strong dipole–dipole interactions [67].

The positive values of α_P^E indicate the presence of weak interactions between the participating components of the mixtures while negative values of α_P^E account for strong interactions between the participating components [68]. Fig. 11 shows negative values of α_P^E in the whole composition range and at all investigated temperatures for the binary mixture in study. This supports the existence of strong interactions between the constituent molecules in binary solution.

The values of excess functions $(\frac{\partial V_m^E}{\partial T})_P$ and $(\frac{\partial H_m^E}{\partial P})_{T=298.15K}$ were given in Table 7. The values of $(\frac{\partial V_m^E}{\partial T})_P$ and $(\frac{\partial H_m^E}{\partial P})_T$ have similar variation with the mole fraction and temperature but with opposite sign. The $(\frac{\partial V_m^E}{\partial T})_P$ values for the studied mixtures are negative. This may be due to strong

Table 6
Partial ($\overline{V}^{\infty}_{m,1}$) and excess partial molar volumes ($\overline{V}^{E,\infty}_{m,1}$) of [Emim][$EtSO_4$] at infinite dilution in 2-ethoxyethanol at T = (298.15, 308.15, 318.15 and 328.15) K.

Temp/K	$\overline{V}^{\infty}_{m,1}$	$\overline{V}^{E,\infty}_{m,1}$
	/(10^{-6} m^3 mol^{-1})	
298.15	185.4138	−5.7008
308.15	185.7556	−6.4321
318.15	186.0034	−7.2367
328.15	185.9351	−8.3572

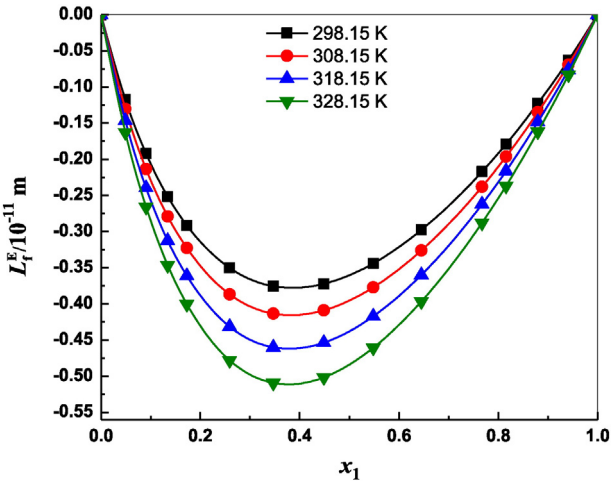

Fig. 5. Plots of excess free length (L_f^E) against mole fraction of [Emim][$EtSO_4$] with 2-ethoxyethanol at different temperatures.

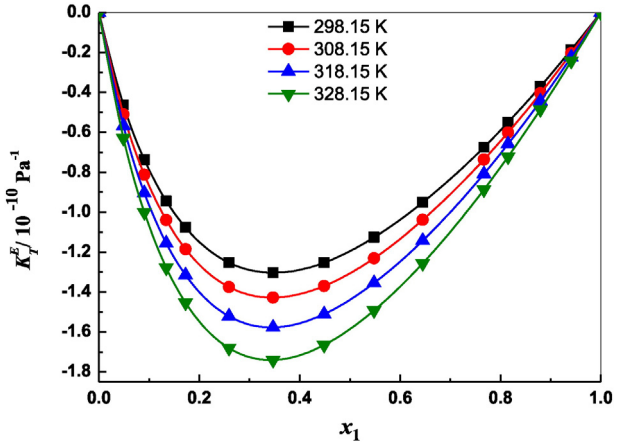

Fig. 6. Plots of excess isothermal compressibility (κ_T^E) against mole fraction of [Emim][$EtSO_4$] with 2-ethoxyethanol at different temperatures.

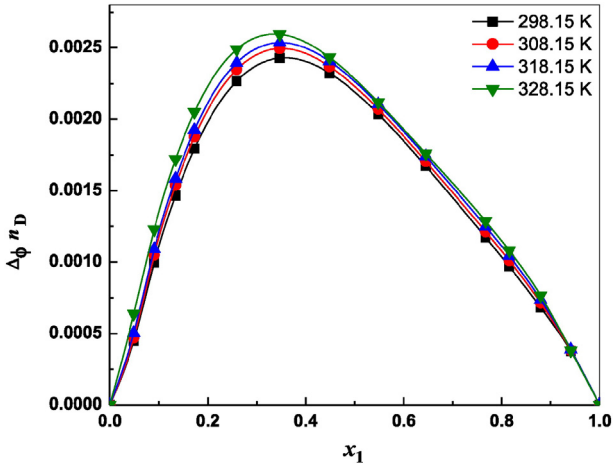

Fig. 8. Plots of deviation in refractive index ($\Delta_\varnothing n_D$) against mole fraction of [Emim][$EtSO_4$] with 2-ethoxyethanol at different temperatures.

interactions existing between the unlike molecules of the mixture [36]. The isothermal pressure coefficient of excess molar enthalpy $(\frac{\partial H_m^E}{\partial P})_{T=298.15K}$ has positive values in the whole composition range. This reflects increase in the attraction forces between two components of this mixture by increasing pressure. Therefore contraction in the volume of the mixture is possible by increasing pressure [69].

The presence of strong interactions in the system which was concluded from the above inferences of derived excess/deviation parameters that are well supported by IR studies. The unique properties of imidazolium cations are found in the electronic structure of the aromatic cations. The electronic structure of these salts contain delocalized 3-center-4-electron configuration across the N_1–C_2–N_3 moiety, a double bond between C_4 and C_5 at the opposite side of the ring, and a weak delocalization in the central region [70]. The hydrogen atoms C_2–H, C_4–H, and C_5–H carry almost the same charge, but carbon C_2 is positively charged owing to the electron deficit in the CN bond, whereas C_4 and C_5 are practically neutral. The resulting acidity of the hydrogen atoms is the key to understand the properties of these ionic liquids. The hydrogen on the C_2 carbon (C_2–H) has been shown to bind specifically with solute molecules [71,72].

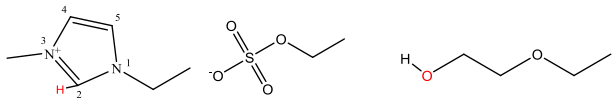

Infrared transmittance recorded from 650 cm^{-1} to 4000 cm^{-1} (Fig. 12) in order to study the effects of molecular interactions on the 1-ethyl-3-methylimidazolium cation the CH stretching region between 2800 and 3200 cm^{-1} is analyzed. For [Emim][$EtSO_4$], the signals in this region can be split into two parts: signals between 3000 $cm^{-1}$and 3200 cm^{-1} can be assigned to CH modes predominantly originating from the aromatic imidazolium ring, from C_2–H and $C_{4,5}$–H stretching frequencies [73]. The signals between 2800 $cm^{-1}$and 3000 cm^{-1} result from aliphatic CH groups in the ethyl and methyl moieties [74–76]. The C_2–H vibrational frequency (3103.5 cm^{-1}) is shifted by about 47 cm^{-1} to lower frequencies than the C_4–H and C_5–H stretches (3150.5 cm^{-1}) due to its stronger acidic character. As we have observed for the cationic aromatic CH, the frequency shows (Table 8) a blue-shift that is observed by the addition of 2-ethoxyethanol to [Emim][$EtSO_4$]. The blue shifts of C_2–H and $C_{4,5}$–H suggest that the aromatic C–H experiences different hydrogen bonding interactions in the mixture as compared with that in the pure [Emim][$EtSO_4$]. In pure [Emim][$EtSO_4$], the C–H bonds in imidazolium cation experience less covalent character as there exists a strong hydrogen bond between imidazolium aromatic C–H hydrogen and nearest oxygen atoms of ethyl sulfate anions. By the addition of 2-ethoxyethanol which interacts with existing ion pairs and breaks the strong hydrogen bonding attractions between imidazolium

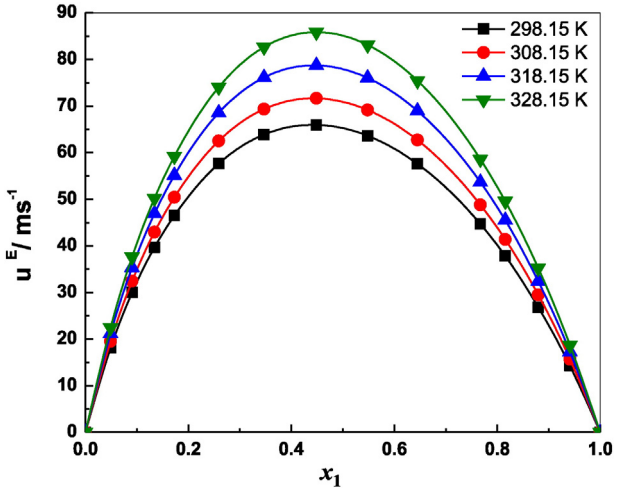

Fig. 7. Plots of excess ultrasonic speed of sounds (u^E) against mole fraction of [Emim][$EtSO_4$] with 2-ethoxyethanol at different temperatures.

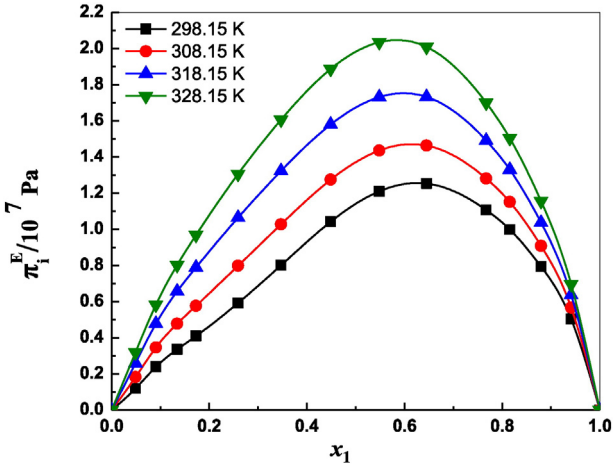

Fig. 9. Plots of excess internal pressure (π_i^E) against mole fraction of [Emim][$EtSO_4$] with 2-ethoxyethanol at different temperatures.

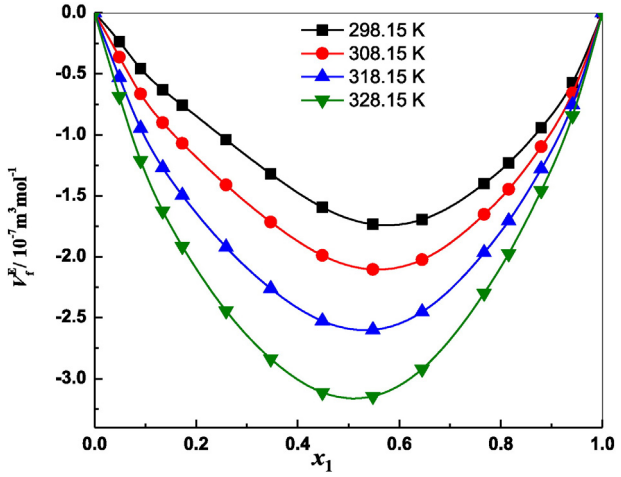

Fig. 10. Plots of excess free volume (V_f^E) against mole fraction of [Emim][$EtSO_4$] with 2-ethoxyethanol at different temperatures.

Table 7

The values of excess functions $(\frac{\partial V_m^E}{\partial T})_P$ and $(\frac{\partial H_m^E}{\partial P})_{T=298.15K}$ against mole fraction of [Emim][$EtSO_4$].

x_1	$(\frac{\partial V_m^E}{\partial T})_P$ /10^{-9} m^3 mol^{-1} K^{-1}	$(\frac{\partial H_m^E}{\partial P})_{T=298.15K}$ /10^{-6} J mol^{-1} Pa^{-1}
0.00000	0.0000	0.0000
0.04876	−3.6513	0.8440
0.09058	−5.9160	1.3706
0.13425	−7.5967	1.7652
0.17272	−8.6106	2.0032
0.25898	−9.7126	2.2491
0.34705	−9.7273	2.2575
0.44890	−8.9530	2.1111
0.54838	−7.7404	1.8725
0.64522	−6.2915	1.5618
0.76737	−4.1903	1.0566
0.81543	−3.3047	0.8303
0.87976	−2.1015	0.5195
0.94121	−0.9805	0.2350
1.00000	0.0000	0.0000

aromatic C–H hydrogen and oxygen atoms of ethyl sulfate anions. This leads to the strengthening of the covalent character of C–H bonds in imidazolium cation and blue shift was observed in the frequencies of imidazolium C–H stretching vibrations. Similar types of interactions were observed in binary mixtures of imidazolium ionic liquids with molecular solvents [77–85].

In the case of $[EtSO_4]^-$ anion IR spectra in the range from 880 to 940 cm^{-1} are analyzed. The peak centered at 912.2 cm^{-1} in the pure RTIL that can be assigned to O–S–O stretching and C–C stretching in the anion. The transmittance decreases with increasing 2-ethoxyethanol mole fraction which indicates the presence of interactions of alkyl hydrogen of 2-ethoxyethanol with $[EtSO_4]^-$ anion [82]. Pure 2-ethoxyethanol has no peak in this range.

Upon addition of 2-ethoxyethanol, the hydroxyl oxygen and alky hydrogen of 2-ethoxyethanol start forming hydrogen bonds with imidazolium aromatic CH hydrogen and oxygen atoms of ethyl sulfate anion respectively. With further addition of 2-ethoxyethanol, significantly weaken inter ionic interactions and eventually initiate ion pair dissociation. Once the individual ions are released, the ions are rapidly saturated with 2-ethoxyethanol.

It is found that hydrogen bonds exist widely in such systems which play a key role towards the stability and miscibility of the [Emim][$EtSO_4$] + 2-ethoxyethanol binary system. The interaction mechanism of 2-ethoxyethanol molecules with the cation and anion is very different in nature. The C–H groups in the imidazolium ring and oxygen atoms in the ethyl sulfate anion are characteristic groups interacting with 2-ethoxyethanol molecules. By studying ATR-FTIR, it can be concluded that C–H groups in the 1-ethyl-3-methyl-imidazolium cation undergo weakened hydrogen bonding interactions under increasing 2-ethoxyethanol concentration. But 2-ethoxyethanol has enough hydrogen bonding interactions with [Emim][$EtSO_4$] to get complete miscibility and solvation of cations and anions in the ionic liquid. Hence, it can be assumed that the hydrogen bonds between the ionic liquid [Emim][EtSO4] and 2-ethoxyethanol are responsible to make a remarkable contraction in the volume of the mixture.

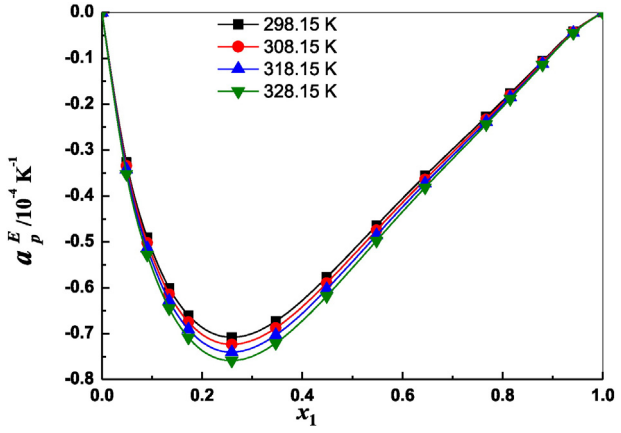

Fig. 11. Plots of excess isobaric thermal expansion coefficient (α_P^E) against mole fraction of [Emim][$EtSO_4$] with 2-ethoxyethanol at different temperatures.

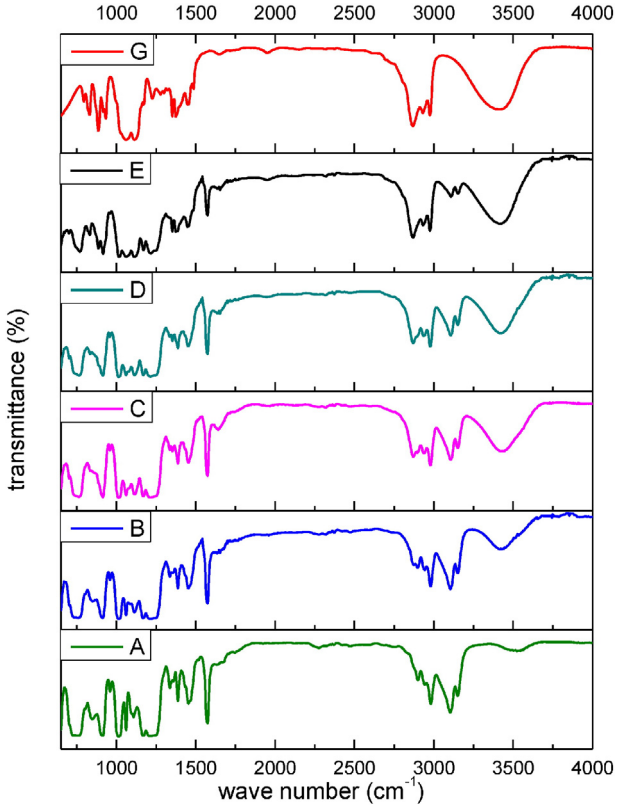

Fig. 12. Infrared spectra A- Pure [Emim][$EtSO_4$], mole fraction of 2-ethoxyethanol in [Emim][$EtSO_4$] (B-0.23263,C-0.45162, D-0.55110, E-0. 0.82728), F- Pure 2-ethoxyethanol.

Table 8
Infrared transmittance wave numbers (cm^{-1}) between 2800 to 3200 of [Emim][$EtSO_4$] in 2-ethoxyethanol at room temperature and P = 0.1 MPa.

Mole fraction of [Emim][$EtSO_4$]	Mole fraction of 2-ethoyethanol	C_2–H stretching	$C_{4,5}$–H stretching
1.00000	0.00000	3103.5	3150.5
0.76737	0.23263	3104.9	3150.6
0.54838	0.45162	3106.9	3150.7
0.44890	0.55110	3106.9	3150.7
0.17272	0.82728	3107.7	3151.8
0.00000	1.00000	–	–

5. Conclusions

Densities, ultrasonic speed of sounds and refractive indices for binary liquids of [Emim][EtSO4] with 2-ethoxyethanol have been measured experimentally over the entire composition range at T = (298.15/308.15/318.15/and 328.15) K. From the experimental data, parameters such as V_m^E, L_f^E, u^E, κ_T^E, V_f^E, α_P^E and $\Delta_\phi n_D$ have been evaluated. The excess and deviation properties have been fitted to Redlich–Kister type polynomial and corresponding standard deviations have been calculated. In the present binary liquid system of [Emim][EtSO4] with 2-ethoxyethanol, the observed negative values of V_m^E, L_f^E, κ_T^E,V_f^E,α_P^E and positive values of u^E, π_i^E and $\Delta_\phi n_D$ clearly indicate the dominance of strong attractive forces. The order of strong interactions follows: (298.15 < 308.15 < 318.15 < 328.15) K. The observed lower partial molar volumes in the liquid mixture when compared to the respective molar volumes of pure components also support the presence of strong interactions in the system. The negative $\left(\frac{\partial V_m^E}{\partial T}\right)_P$ values and the positive values of isothermal pressure coefficient of excess molar enthalpy $\left(\frac{\partial H_m^E}{\partial P}\right)_{T=298.15K}$ suggest the existence of strong interactions between the unlike molecules of the mixture. IR spectral studies clearly indicate the formation of hydrogen bonds giving rise to strong interaction between [Emim][EtSO4] with 2-ethoxyethanol.

References

[1] A. Bösmann, L. Datsevich, A. Jes, A. Lauter, C. Schmitz, P. Wasserscheid, Chem. Commun. 23 (2001) 2494–2495.
[2] Maciej Galiński, Andrzej Lewandowski, Izabela Stępniak, Electrochim. Acta 51 (2006) 5567–5580.
[3] Martyná Earle, J. Kennethá, R. Seddon, Christopherá J. Adams, Chem. Commun. 19 (1998) 2097–2098.
[4] T. Fischer, A. Sethi, T. Welton, J. Woolf, Tetrahedron Lett. 40 (1999) 793–796.
[5] P. Snedden, A.I. Cooper, K. Scott, N. Winterton, Macromolecules 36 (2003) 4549–4556.
[6] V. Natalia Plechkova, Kenneth R. Seddon, Chem. Soc. Rev. 37 (2008) 123–150.
[7] J.A. Laszlo, D.L. Compton, Biotechnol. Bioeng. 75 (2001) 181–186.
[8] M. Francesca Kerton, Ray Marriott, R. Soc. Chem. (2013).
[9] B.E. Gurkan, J. C.de la Fuente, E.M. Mindrup, L.E. Ficke, B.F. Goodrich, E.A. Price, J.F. Brennecke, J. Am. Chem. Soc. 132 (2010) 2116–2117.
[10] L.P. Rebelo, J.N. Canongia Lopes, J.M. Esperança, E. Filipe, J. Phy. Chem. B 109 (2005) 6040–6043.
[11] J.G. Huddleston, A.E. Visser, W.M. Reichert, H.D. Willauer, G.A. Broker, R.D. Rogers, Green Chem. 3 (2001) 156–164.
[12] Tetsuo Nishida, Yasutaka Tashiro, Masashi Yamamoto, J. Fluor. Chem. 120 (2003) 135–141.
[13] K.O.E.L. Mihkel, Proc. Est. Acad. Sci., Chem. 49 (2000) 145–155.
[14] D. John Holbrey, Kenneth R. Seddon, J. Chem. Soc. Dalton Trans. 13 (1999) 2133–2140.
[15] P. Bonhote, A.P. Dias, N. Papageorgiou, K. Kalyanasundaram, M. Grätzel, Inorg. Chem. 35 (1996) 1168–1178.
[16] George Law, Philip R. Watson, Langmuir 17 (2001) 6138–6141.
[17] H.L. Ngo, K. LeCompte, L. Hargens, A.B. McEwen, Thermochim. Acta 357 (2000) 97–102.
[18] P. Izák, N.M. Mateus, C.A. Afonso, J.G. Crespo, Sep. Purif. Technol. 41 (2005) 141–145.
[19] M.J. Muldoon, S.N.V.K. Aki, J.L. Anderson, J.K. Dixon, J.F. Brennecke, J. Phys. Chem. B 111 (2007) 9001–9009.
[20] J.L. Anderson, J.K. Dixon, J.F. Brennecke, Acc. Chem. Res. 40 (2007) 1208–1216.
[21] I. Khan, M.L. Batista, P.J. Carvalho, L.M. Santos, J.R. Gomes, J.A. Coutinho, J. Phys. Chem. B 119 (2015) 10287–10303.
[22] H. Passos, I. Khan, F. Mutelet, M.B. Oliveira, P.J. Carvalho, L.M.N.B.F. Santos, C. Held, G. Sadowski, M.G. Freire, J.A.P. Coutinho, Ind. Eng. Chem. Res. 53 (2014) 3737–3748.
[23] P.J. Carvalho, I. Khan, A. Morais, J.F.O. Granjo, N.M.C. Oliveira, L.M.N.B.F. Santos, J.A.P. Coutinho, Fluid Phase Equilib. 354 (2013) 156–165.
[24] I. Khan, M. Taha, P. Ribeiro-Claro, S.P. Pinho, J.A.P. Coutinho, J. Phys. Chem. B 118 (2014) 10503–10514.
[25] I. Khan, K.A. Kurnia, T.E. Sintra, J.A. Saraiva, S.P. Pinho, J.A.P. Coutinho, Fluid Phase Equilib. 361 (2014) 16–22.
[26] I. Khan, K.A. Kurnia, F. Mutelet, S.P. Pinho, J.A. Coutinho, J. Phys. Chem. B 118 (2014) 1848–1860.
[27] H. Passos, M.G. Freire, J.A.P. Coutinho, Green Chem. 16 (2014) 4786–4815.
[28] Electrochemical Aspects of Ionic Liquids, 2 ed. John Wiley & Sons, Inc., New Jersey, 2005.
[29] L. Alonso, A. Arce, M. Francisco, A. Soto, Fluid Phase Equilib. 270 (2008) 97–102.
[30] L. Alonso, A. Arce, M. Francisco, A. Soto, J. Solut. Chem. 37 (2008) 1355–1363.
[31] A. Kokorin, Ionic Liquids: Applications and Perspectives, 2011.
[32] M.H. Mabaso, G.G. Redhi, K.G. Moodley, S. African, J. Chemother. 65 (2012) 145–149.
[33] T. Singh, A. Kumar, J. Chem. Thermodyn. 40 (2008) 417–423.
[34] A. Kumar, T. Singh, R.L. Gardas, J.A. Coutinho, J. Chem. Thermodyn. 40 (2008) 32–39.
[35] A. Pal, B. Kumar, Fluid Phase Equilib. 334 (2012) 157–165.
[36] A. Pal, B. Kumar, J. Mol. Liq. 163 (2011) 128–134.
[37] Concise International Chemical Assessment Document 67, World Health Organization, 2009.
[38] E.J. González, B. González, N. Calvar, Á. Domínguez, J. Chem. Eng. Data 52 (2007) 1641–1648.
[39] G. Miaja Gonzalo, J. Troncoso, Luis Romaní, J. Chem. Thermodyn. 4 (1) (2009) 161–166.
[40] J. Lehmann, M.H. Rausch, A. Leipertz, A.P. Fröba, J. Chem. Eng. Data 55 (2010) 4068–4074.
[41] U. Domańska, M. Laskowska, J. Solut. Chem. 37 (9) (2008) 1271–1287.
[42] A.P. Carneiro, O. Rodríguez, C. Held, G. Sadowski, E.A. Macedo, J. Chem. Eng. Data 59 (2014) 2942–2954.
[43] Anantharaj Ramalingam, R.R. Subramanian, A. Arunagiri, J. Innov. Eng. 2 (2) (2014) 6.
[44] A.N. Soriano, B.T. Doma, M.H. Li, J. Taiwan Inst. Chem. Eng. 41 (2010) 115–121.
[45] R. Ge, C. Hardacre, J. Jacquemin, P. Nancarrow, D.W. Rooney, J. Chem. Eng. Data 53 (2008) 2148–2153.
[46] C.P. Pandhurnekar, D.V. Parwate, S.S. Dhondge, J. Mol. Liq. 183 (2013) 94–101.
[47] http://webbook.nist.gov/cgi/cbook.cgi?ID=C110805&Mask=2.
[48] E. Scholz, Karl Fischer Titration, Springer-Verlag, Berlin, 1984.
[49] George C. Benson, Osamu Kiyohara, J. Chem. Eng. Data 21 (1976) 362–365.
[50] G. Douheret, M.I. Davis, J.C.R. Reis, M.J. Blandamer, ChemPhysChem 2 (2001) 148–161.
[51] J.D. Pandey, S.K. Shukla, J. Chhabra, R. Dey, J. Indian Chem. Soc. 81 (2004) 962.
[52] W. Westwater, H.W. Frantz, J.H. Hildebrand, Phys. Rev. 31 (1928) 135.
[53] U. Bianchi, G. Agabio, A. Turturro, J. Phys. Chem. 69 (12) (1965) 4392.
[54] G.A. Few, M. Rigby, J. Phys. Chem. 79 (15) (1975) 1543.
[55] D.D. MacDonald, J.B. Hyne, Can. J. Chem. 49 (1971) 611 (and ib. 2637).
[56] E. Zorębski, Mol. Quant. Acoust. 26 (2005) 317.
[57] G. Douheret, A. Khadir, A. Pal, Thermochim. Acta 142 (1989) 219.
[58] G. Douheret, M.I. Davis, J.C.R. Reis, M.J. Blandamer, ChemPhysChem 2 (2001) 148.
[59] Ranjan Dey, A.K. Singh, J.D. Pandey, J. Mol. Liq. 124 (2006) 121.
[60] Sk.Md. Nayeem, M. Kondaiah, K. Sreekanth, D. Krishna Rao, J. Mol. Liq. 207 (2015) 286–293.
[61] Sk.Md. Nayeem, Kondaiah M., K. Sreekanth, D. Krishna Rao, Arab. J. Chem. (2015), http://dx.doi.org/10.1016/j.arabjc.2015.08.005.
[62] S. Govardhana Rao, T. Madhu Mohan, T. Vijaya Krishna, T. Srinivasa Krishna, B. Subba Rao, J. Chem. Eng. Data 60 (2015) 886–894.
[63] I. Ismael, G. de la Fuente, J.A. González, J.C. Cobos, J. Mol. Liq. 136 (1) (2007) 117–127.
[64] Sk.Md. Nayeem, Kondaiah M., K. Sreekanth, D. Krishna Rao, J. Thermodyn. (2014), http://dx.doi.org/10.1155/2014/487403.
[65] F.N. Anwar Ali, Tariq M., Int. J. Thermophys. 30 (2009) 464–474.
[66] E. Vercher, J.L. Francisco, A. Vicenta González, J.M. Pablo, O. Vicent, M.A. Antoni, J. Chem. Thermodyn. 90 (2015) 174–184.
[67] K. Rajagopal, S. Chenthilnath, Chin. J. Chem. Eng. 18 (2010) 804–816.
[68] A. Ali, M. Tariq, J. Pure. Appl. Ultrason. 28 (2006) 99.
[69] F. Kermanpour, H.Z. Niakan, J. Chem. Thermodyn. 48 (2012) 129–139.
[70] P.A. Hunt, B. Kirchner, T. Welton, Chem. Eur. J. 12 (2006) 6762–6775.
[71] A. Aggarwal, N.L. Lancaster, A.R. Sethi, T. Welton, Green Chem. 4 (5) (2002) 517–520.
[72] V. Znamenskiy, M.N. Kobrak, J. Phys. Chem. B 108 (2004) 1072–1079.
[73] N.R. Dhumal, H.J. Kim, J. Kiefer, J. Phys. Chem. A 115 (2011) 3551–3558.
[74] J.C. Lassègues, J. Grondin, D. Cavagnat, P. Johansson, J. Phys. Chem. A 113 (2009) 6419–6421.
[75] J.C. Lassègues, J. Grondin, D. Cavagnat, P. Johansson, J. Phys. Chem. A 114 (2009) 687–688.
[76] J. Grondin, J.C. Lassègues, D. Cavagnat, T. Buffeteau, P. Johansson, R. Holomb, J. Raman, Spectrum 42 (2011) 733–743.
[77] Y. Chen, Y. Cao, X. Sun, T. Mu, J. Mol. Liq. 190 (2014) 151–158.
[78] H. He, H. Chen, Y. Zheng, X. Zhang, X. Yao, Z. Yu, S. Zhang, Aust. J. Chem. 66 (2013) 50–59.

[79] Y.Z. Zheng, N.N. Wang, J.J. Luo, Y. Zhou, Z.W. Yu, Phys. Chem. Chem. Phys. 15 (2013) 18055–18064.
[80] J. Stejskal, J. Dybal, M. Trchová, Synth. Met. 197 (2014) 168–174.
[81] K. Noack, A. Leipertz, J. Kiefer, J. Mol. Struct. 1018 (2012) 45–53.
[82] Y. Umebayashi, J.C. Jiang, K.H. Lin, Y.L. Shan, K. Fujii, S. Seki, H.C. Chang, J. Chem. Phys. 23 (2009) 131.
[83] T. Shimomura, K. Fujii, T. Takamuku, Phys. Chem. Chem. Phys. 12 (2010) 12316–12324.
[84] M. López-Pastor, M.J. Ayora-Cañada, M. Valcárcel, B. Lendl, J. Phys. Chem. B 110 (2006) 10896–10902.
[85] J. Kiefer, M.M. Molina, K. Noack, ChemPhysChem 13 (2012) 1213–1220.